Published by Nigerian Society of Physical Sciences. Hosted by FLAYOO Publishing House LTD

Recent Advances in Natural Sciences

Journal Homepage: https://flayoophl.com/journals/index.php/rans

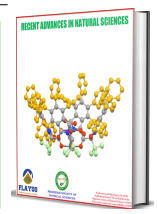

Environmental and health impacts of coal occurrence and exploitation in Akunza mighili, North central Nigeria

S. Iyakwari, S. Aliyu*, F. O. Balogun[1], I. Y. Anzaku, N. Musa

Federal University of Lafia, P.M.B 146, Nasarawa State, Nigeria

ARTICLE INFO

Article history:
Received: 21 June 2025
Received in revised form: 09 September 2025
Accepted: 05 December 2025
Available online: 31 December 2025

Keywords: Akunza mighili, Coal, T_{max}, Heavy metal pollution index, X-ray fluorescence

DOI:10.61298/rans.2026.3.2.217

ABSTRACT

Akunza Mighili is a community in the outskirts of Lafia widely known for extensive coal mining activities. However, no assessment has been conducted on the impact of this mining on the environment and health hazards. This research aims to investigate the environmental and health impacts of coal exploitation in Akunza Mighili. Five representative rock samples were collected during field mapping and analyzed to determine their elemental and mineralogical constituents using X-ray fluorescence (XRF) and X-ray diffraction (XRD). Additionally, two coal samples were subjected to rock eval pyrolysis. A total of twenty groundwater samples were collected and analyzed using Atomic Absorption Spectroscopy (AAS). Measurement of groundwater physical parameters was also conducted during the field mapping. Field results indicated that the area primarily consists of shale interbedded with coal seams, ferruginous sandstone, ferruginous siltstone, and minor occurrences of mudstone. Based on the XRD and XRF results, graphite is the dominant mineral in coal while SO_3 and SiO_2 represent the dominant major oxides. The coal samples in the area are immature for oil generation based on their maximum pyrolysis temperature (T_{max}). In the groundwater of the area, the order of parameters is pH > Total Dissolved Solids (TDS) > Temperature (T) > Electrical Conductivity (EC), while the concentration of heavy metals follows this order: Fe > Zn > Cu > Co > Cd > Mn > Cr > Ni > Pb > Hg. The assessment of heavy metal pollution indicated that the groundwater in the area is significantly polluted, which poses serious health risks.

1. INTRODUCTION

Coal is an important component of global energy production, which has driven industrialization and economic development over the years [1, 2]. It served as a major source of fuel used in the generation of electricity, contributing to about 36% of the world's electricity [3]. Despite the benefits of coal, exploitation activities negatively impact the natural environment and human health. Globally, well-documented consequences of coal exploitation include groundwater pollution, climate change, deforestation, and degradation of air quality [4, 5].

In countries with an abundance of coal deposits, like Nigeria, exploitation activities significantly impact the environment [6]. Open-pit and underground mining systems are widely recognized to degrade surficial features such as topsoil and vegetation, making the land unsuitable for agricultural use [7, 8]. This damage is in addition to subsidence and release of heavy metals

*Corresponding author Tel. No: +234-703-230-0085.
e-mail: glgship@gmail.com (S. Aliyu)

and toxic trace elements into nearby water bodies [9, 10]. Non-selective disposal of tailings is another issue of serious concern for the environment. Moreover, the environment receives large quantities of dust and other toxic pollutants, especially during coal exploitation and burning [5–12]. These pollutants, comprising silica dust, sulphur dioxide, nitrogen oxides, and particulate matter, affect the respiratory and cardiovascular systems, among other health issues [11–13].

Evaluating the environmental impact of mining requires the use of specialized techniques capable of detecting the mineralogy and chemical compositions of soil and rocks, as well as the chemical constituents of groundwater [14–16]. These parameters can be effectively and comprehensively monitored using a combination of X-ray Diffraction (XRD), X-ray Fluorescence (XRF), and Atomic Absorption Spectrometry (AAS) techniques [17, 18]. The XRD is efficient in assessing potentially harmful minerals and crystalline phases in rocks and mine tailings, respectively [19–21]. For instance, XRD detects sulphide minerals like pyrite and chalcopyrite, which significantly contribute to the formation of Acid Mine Drainage (AMD) [22, 23]. The XRF is a rapid and non-destructive method used to determine the composition of toxic heavy metals and trace elements in environmental samples, including dust from mining sites [24, 25]. On the other side, AAS is another sensitive technique often used to identify and quantify toxic heavy metal concentrations, such as Pb, As, Cr, Ni, Zn, and Cu, in water samples [26–28].

This research aims to investigate the environmental and health impacts associated with coal exploitation in Akunza Mighili, North Central Nigeria, focusing primarily on groundwater quality and its effects on the local community. The outcome of this research work will address the gap in knowledge with respect to the environmental and health impacts of coal exploitation in the study area.

2. MATERIALS AND METHODS

2.1. LOCATION, PHYSIOGRAPHY AND GEOLOGICAL SETTING

Akunza Mighili is located in Lafia, north-central Nigeria, situated within latitudes 8° 24’ 00"N to 8° 30’ 00"N and longitudes 8° 32’ 30"E to 8° 34’ 59"E (Figure 2). The area has a low-undulating topography and a dendritic drainage pattern, drained by the River Amba and its tributaries. It is situated within the tropical savannah climate, with the dry season commencing from October to April, while the wet season starts in April and lasts until around October and November. The mean annual rainfall, humidity, and temperature values are 1000mm, 70%, and 30°C, respectively [29]. Vegetation is typical of the tropical Guinea savanna, composed of scattered trees, shrubs, and grasses.

The area extends across two formations: the Agwu Formation and the Lafia Formation. However, The Akunza Mighili Coal Mine falls within the Agwu formation in the Middle Benue Trough. The Middle Benue Trough is one of the subdivisions of the Benue Trough of Nigeria. It is subdivided into six formations in order of age: Asu River Group, Awe Formation, Keana Formation, Ezeaku Formation, Awgu Formation, and Lafia Formation [30, 31]. The Awgu Formation is the second youngest formation in the Middle Benue Trough, precisely Late Turonian-Coniacian in age. It marks the end of marine sedimentation in the Middle Benue Trough, overlying the Ezeaku Formation

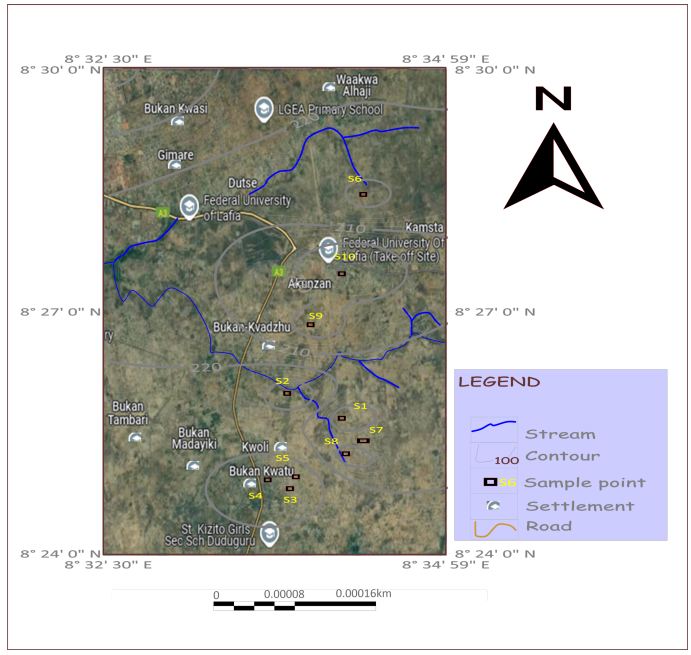

Figure 1. Location and sample location of the study area.

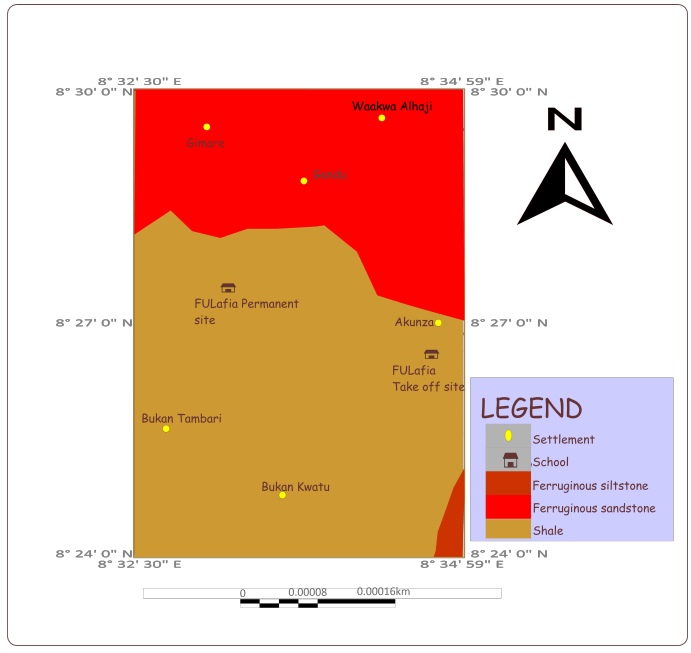

Figure 2. Geological map of the study area.

conformably, which is characterized by coal seams of variable thickness [30, 31]. The formation dominantly consists of shales [30, 32]. The Lafia Formation is Maastrichtian in age, overlying the Agwu Formation unconformably [33]. It consists of continental sediments (ferruginous sandstones, siltstones, and claystones) and is marked by prominent ferruginization [34–36].

2.2. FIELDWORK, SAMPLING AND ANALYTICAL METHODS

Geological fieldwork was conducted within the Akunza Mighili Coal mine and the entire research area to assess the various rock units in the area. The location of each rock unit was taken using

Figure 3. Field exposure of shale and coal seams.

Figure 4. Exposed section of shale.

Figure 5. Ferruginous sandstone.

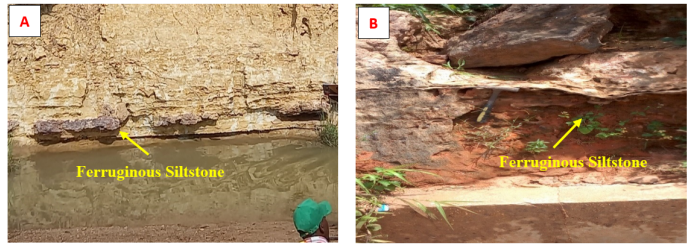

Figure 6. Exposed sections of ferruginous siltstone.

the Geographic Positioning System (GPS). Similarly, fresh rock samples and groundwater samples were obtained during the field mapping. Five representative rock samples comprising shale, coal, ferruginous sandstone, ferruginous siltstone and mudstone were selected for determination of major oxides and mineralogical composition using the X-ray Fluorescence (XRF) and X-ray Diffraction (XRD) techniques accordingly. These analyses were both conducted at the National Steel Raw Materials Agency, Kaduna. Two other representative coal samples were collected for rock eval pyrolysis, carried out using the Rock Eval 6 analyzer, in Lighthouse Petroleum Engineering Company Limited, Effurun, Delta State, Nigeria.

A total of twenty (20) groundwater samples were collected for determination of heavy metal cations, using 1L plastic bottles. The samples were acidified with a concentrated nitric acid (HNO3) to homogenize the sample and prevent adsorption of cations to the walls of the sampling bottles. The physical parameters of the collected water samples-pH, electrical conductivity (EC), total dissolved solids (TDS), and temperature-were measured in the field using the Hanna multimeter. Chemical analysis of the groundwater samples for heavy metals (Fe, Zn, Cd, As, Cu, Mn, Co, Hg, Cr, Ni, Pb) was conducted in the Federal Ministry of Water Resources, using the Atomic Absorption Spectrometry (AAS).

2.3. ASSESSMENT OF HEAVY METAL POLLUTION

The pollution status of groundwater in the research area with respect to heavy metals was determined using a combined analysis of various pollution indices, including the Heavy Metal Pollution Index (HPI), Modified Heavy Metal Pollution Index (mHPI), Degree of Contamination (Dc), and Heavy Metal Evaluation Index (HEI). These indices are effective methods of assessing the heavy metal pollution levels of groundwater associated with coal mines [37, 38].

2.3.1. Heavy Metal Pollution Index (HPI)

The Heavy Metal Pollution Index reveals the collective impact of heavy metals in groundwater [39]. It is calculated by assigning a weightage (*Wi*) to individual heavy metals analyzed, expressed

Table 1. Major oxide composition of rocks in the study area (wt.%).

Parameter	Coal	Shale	Mudstone	Ferruginous sandstone	Ferruginous siltstone
MgO	6	-	-	-	-
SiO_2	27.97	55.97	48.78	31.36	49.45
V_2O_3	0.21	0.23	0.18	0.1	0.06
Cr_2O_3	0.04	0.04	0.03	0.03	0.12
MnO	0.25	0.14	0.16	0.31	0.02
Fe_2O_3	9.19	13.15	20.46	52.33	40.17
Ag_2O	0.09	0.07	0.04	-	-
BaO	-	0.08	-	0.13	0.16
CuO	0.4	0.06	0.06	0.04	0.03
Nb_2O_3	0.1	0.03	0.03	-	-
P_2O_5	-	-	-	0.15	0.83
SO_3	30.26	0.65	3.16	0.18	0.35
CaO	8.26	0.47	1.28	0.26	0.08
K_2O	0.02	2.94	2.38	1.9	0.06
Al_2O_3	12.31	21.76	20.42	11.71	8.03
Ta_2O_5		0.02	0.02	0.01	0.01
TiO_2	4.41	4.05	2.72	1.15	0.39
SnO_2	-	-	-	0.07	-
ZrO_2	0. 13	0.26	0.14	-	-
ZnO	0.21	0.04	0.05	0.02	0.01
Min	0.02	0.02	0.02	0.01	0.01
Max	30.26	55.97	48.78	52.33	49.45
Mean	7.64	8.20	8.26	8.44	8.77

Table 2. Bulk mineralogy of rocks in the study area.

Coal		Shale		Mudstone		Ferruginous sandstone		Ferruginous siltstone	
Mineral	(%)	Mineral	(%)	Mineral	(%)	Mineral	(%)	Mineral	(%)
Quartz	26	Quartz	54	Quartz	52	Quartz	27	Quartz	40
Epsomite	10.1	Anatase	5.9	Anatase	6	Anatase	1.3	Goethite	53
Osumilite	0.8	Goethite	13.5	Goethite	10	Goethite	58	Microcline	7.4
Anhydrite	13.9	Orthoclase	27	Orthoclase	22	Orthoclase	13.6	–	–
Alunogen	9	–	–	Anhydrite	9	–	–	–	–
Graphite	40	–	–	–	–	–	–	–	–

Table 3. Results of coal pyrolysis.

Sample ID	TOC	S1	S2	HI	OI	*T*max.
CS1	64.97	1.42	240.62	318	7	409
CS2	70.31	0.28	153.21	219	7	405
Average	67.64	0.85	196.92	293.5	7	407

Where TOC = Total Organic Carbon (wt %), HI = hydrogen Index (mg HC/g TOC), OI = Oxygen Index (mg CO_2/g TOC), *T*max = Temperature of maximum HC generated during pyrolysis, *S1* = Free Indigenous HC (mg HC/g rock), *S2* = Pyrolysable HC (mg HC/g rock).

in values inversely proportional to their standard limits [40–42]. The HPI was computed using the functions [38, 40]:

$$\mathrm{HPI} = \frac{\sum_{i=1}^{n} W_i Q_i}{\sum_{i=1}^{n} W_i}, \tag{1}$$

where *Wi* is the unit weightage of the i^{th} parameter, *Qi* represents the sub-index value of the i^{th} parameter, and *n* is the number of parameters being assessed. The sub-index (*Qi*) was achieved using equation 2:

$$Q_i = \left(\frac{M_i - I_i}{S_i - I_i}\right) \times 100, \tag{2}$$

where *Mi* signifies the measured value for the i^{th} parameter, *Ii* stand for ideal value for the i^{th} and *Si* represent standard value of the i^{th} parameter. HPI values (HPI<50) are categorized as low, (HPI 50-100) as medium and HPI>100 as high pollution [40].

2.3.2. Modified heavy metal pollution index (MHPI)

The MHPI involves assigning non-objective weights to heavy metals on the basis of their potential health effect [35]. A unit

Table 4. Physicochemical parameters of groundwater.

Sample ID	pH	EC (mS/cm)	TDS	T	Fe	Zn	Cd	As	Cu	Mn	Co	Hg	Cr	Ni	Pb
S1	8.6	0.52	285	34.3	1.00	0.09	0.003	0.01	0.99	0.10	0.085	BDL	BDL	0.02	0.001
S2	5.8	0.10	76	31.2	0.60	0.80	0.046	BDL	0.09	0.006	0.021	BDL	BDL	0.01	BDL
S3	4.5	0.52	37.1	30.2	0.67	1.02	0.031	BDL	0.90	0.006	0.020	BDL	0.02	0.02	BDL
S4	5.2	0.33	235	30.2	0.69	0.761	0.026	BDL	0.91	0.005	0.021	BDL	BDL	0.01	BDL
S5	5.5	0.58	395	29.9	0.68	1.021	0.043	BDL	0.912	0.005	0.020	BDL	0.02	0.01	BDL
S6	5.5	0.04	35	31.0	0.05	0.872	0.039	BDL	0.10	BDL	0.010	BDL	0.01	BDL	BDL
S7	5.9	0.40	38	32.1	0.04	0.91	0.070	BDL	0.11	BDL	0.010	BDL	0.01	BDL	BDL
S8	6.2	0.20	145	30.9	0.07	0.862	0.055	BDL	0.39	0.007	0.011	BDL	BDL	BDL	BDL
S9	6.4	0.16	123	31.2	0.08	0.22	0.032	BDL	0.41	0.008	0.090	BDL	BDL	BDL	BDL
S10	5.0	0.17	126	38.8	0.45	0.35	0.027	BDL	0.53	0.003	0.080	BDL	0.02	0.01	0.001
S11	6.5	0.61	434	33.8	0.81	0.013	0.001	BDL	0.06	0.010	0.005	BDL	0.03	0.001	BDL
S12	6.6	0.21	150	37.9	0.80	0.013	0.020	BDL	0.05	0.005	0.800	BDL	BDL	0.001	BDL
S13	5.9	0.13	101	32.4	0.82	0.013	0.001	BDL	0.059	0.030	0.005	BDL	0.01	0.001	BDL
S14	6.5	0.19	138	33.6	0.84	0.012	0.001	BDL	0.06	0.020	0.005	BDL	0.01	0.001	BDL
S15	4.9	0.02	0.22	31.1	0.82	0.012	0.001	BDL	0.058	0.020	0.004	BDL	BDL	0.001	BDL
S16	6.0	0.18	131	33.0	0.79	0.013	0.010	BDL	0.06	0.010	0.004	BDL	0.01	0.01	BDL
S17	6.1	0.12	92	32.2	0.81	0.013	0.001	BDL	0.061	0.010	0.004	BDL	BDL	0.001	BDL
S18	6.2	0.05	43	34.7	0.22	BDL	BDL	BDL	BDL	BDL	0.001	BDL	BDL	BDL	BDL
S19	6.5	0.05	43	33.5	0.85	0.013	0.001	BDL	0.06	0.020	0.005	BDL	BDL	0.001	BDL
S20	6.0	0.05	41	33.1	0.80	0.013	0.001	BDL	0.063	0.020	0.005	BDL	BDL	0.001	BDL
Min.	4.5	0.02	0.22	29.9	0.04	0.012	0.001	0.01	0.05	0.003	0.001	0.00	0.01	0.001	0.001
Max.	8.6	0.61	434	38.8	1.00	1.021	0.070	0.01	0.99	0.10	0.800	0.00	0.03	0.02	0.001
Average	5.9	0.232	133.42	32.75	0.59	0.37	0.02	0.01	0.31	0.01	0.06	0.00	0.02	0.01	0.001

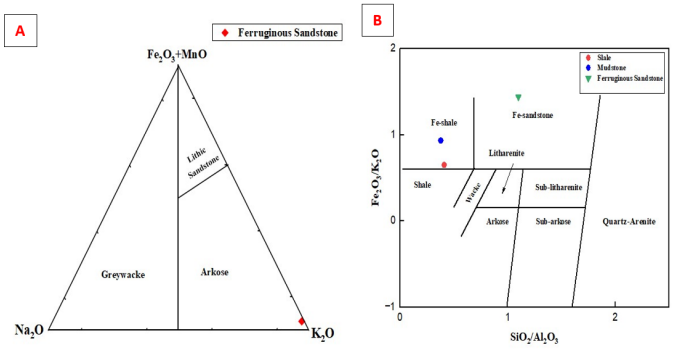

Figure 7. Chemical classifiaction of rocks in the study area: (A) Ternery plot of Fe_2O_3+MgO – Na_2O – K_2O (B) The log (Fe_2O_3/MgO) *vs* (SiO_2/Al_2O_3).

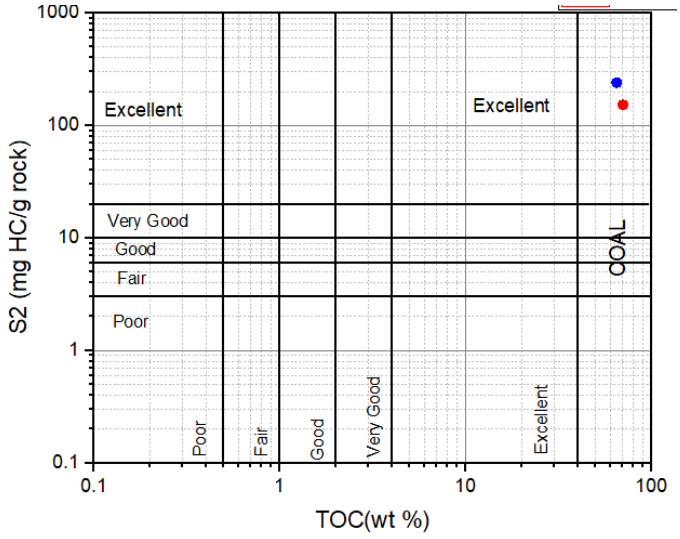

Figure 8. Plot of TOC *vs* S2.

weightage of 1-5 was adopted for the measured heavy metal in the groundwater of the area. The Modified Heavy Metal Pollution Index was evaluated using equations 3 and 4:

$$R_w = \frac{w_i}{\sum_{i=1}^{n} w_i}, \tag{3}$$

$$\text{MHPI} = \sum_{i=1}^{n} \left(\frac{R_w \times M_i}{S_i} \right) \times 100, \tag{4}$$

where *Rw*,*n,* and *Wi* signify the relative weight, number of parameters under investigation, and *unit* weight for the i^{th} parameter respectively. *Mi* represents the monitored value of heavy metals, and *Si* is the upper standard limit for the i^{th} parameters recommended by the WHO [43]. MHPI less than 50 are considered excellent, between 50 and 100 are good, 100 to 200 are considered poor, values ranging from 200 to 300 are very poor, while values above 300 are considered unsuitable for drinking [44].

2.3.3. Degree of Contamination (Dc)

The Degree of Contamination (Dc) indicates the level of contamination of individual heavy metals in groundwater [40, 45]. The Dc values for each heavy metal analyzed were computed, and then the cumulative Dc values of heavy metals in the groundwater samples were obtained by summing the individual contamination values. These were both achieved using equations 5 and

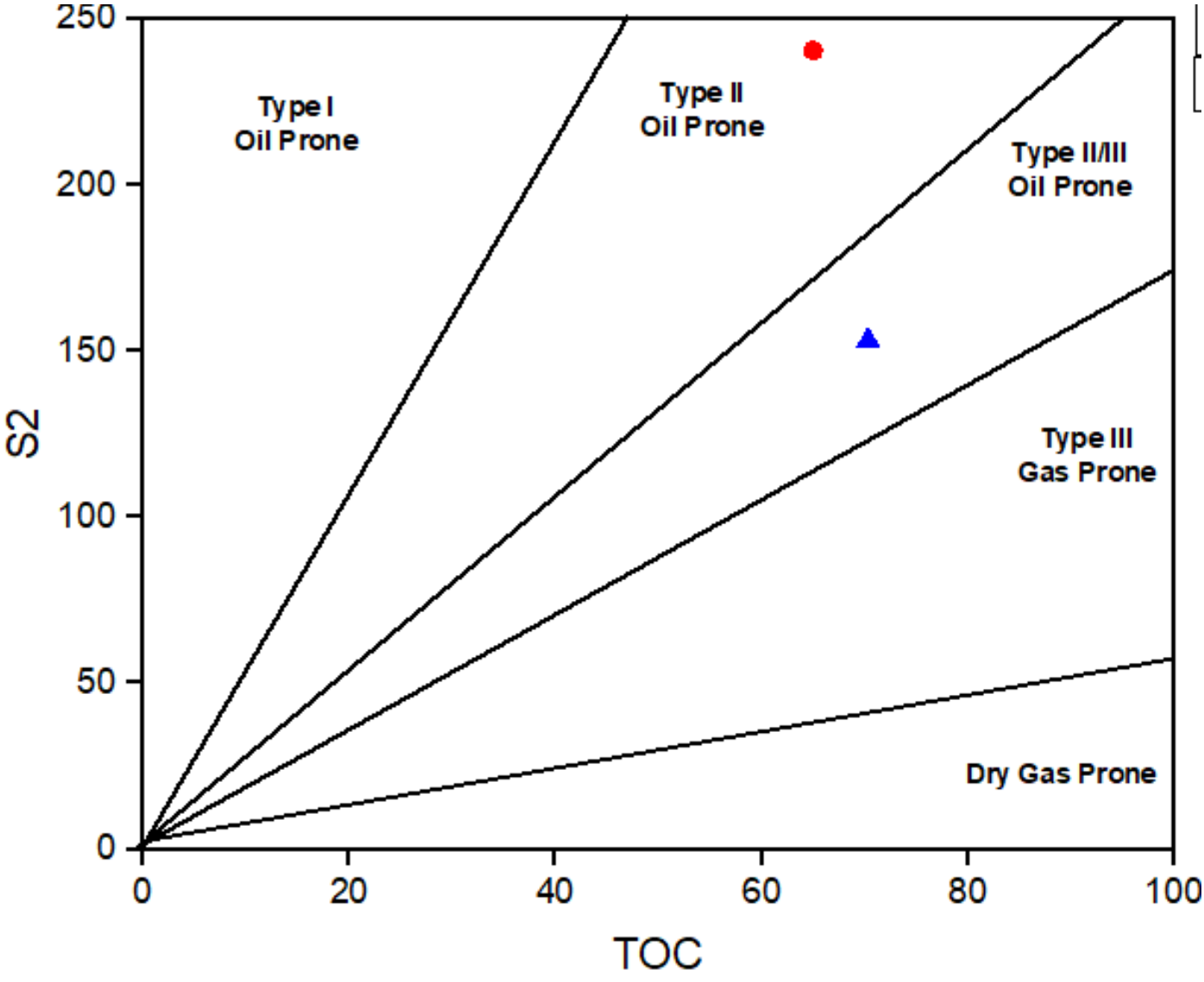

Figure 9. Plot of TOC *vs* S2.

6:

$$C_d = \sum_{i=1}^{n} C_{f_i}, \tag{5}$$

$$C_{f_i} = \frac{C_{A_i}}{C_{N_i}} - 1, \tag{6}$$

$$\mathrm{HEI} = \sum_{i=1}^{n} \frac{H_c}{H_{\mathrm{mac}}}, \tag{7}$$

where *Cfi* stand for the contamination factor of the i^{th} parameter, *CAi* is the monitored value and *CNi* is the maximum recommended threshold by WHO [43]. Dc values are classified as low (Dc<1), medium (Dc 1-3), and high (Dc>3) [40].

2.3.4. Heavy Metal Evaluation Index (HEI)

The Heavy Metal Evaluation Index (HEI) is another metric that provides an overall assessment of water quality with respect to heavy metals. The HEI was calculated using the equation below [38, 40, 45]:

$$\mathrm{HEI} = \sum_{i=1}^{n} \frac{H_c}{H_{\mathrm{mac}}}. \tag{8}$$

The variables *Hc* and *Hmac* denote the measured value and the maximum allowable concentration of the i^{th} parameter, respectively. HEI values (HEI<10) are classified as low, (HEI 10–20) as medium and (HEI>20) as high [40].

3. RESULT AND DISCUSSION

3.1. GEOLOGY OF THE STUDY AREA

The study area is underlain by the Late Turonian-Early Santonian sediments of the coal-bearing Awgu Formation and the Ferruginous-Maastrichtian rocks of the Lafia Formation in the Middle Benue Trough (Figure 3).

Table 5. Heavy metal pollution data.

Sample	HPI	MHPI	HEI	DC
S1	47.5884	55.71709	19.8819	8.46
S2	911.8217	212.7656	20.89286	18.17
S3	1692.808	1308.148	17.40952	14.81
S4	290.4377	134.998	15.32319	12.6
S5	480.0981	210.9035	21.30233	18.71
S6	434.0127	172.4186	15.1859	13.91
S7	778.4474	304.8681	25.50857	24.23
S8	611.532	242.4601	20.88543	19.44
S9	357.6046	152.1551	24.35381	12.75
S10	304.2236	142.232	23.2481	12.95
S11	13.4397	24.64737	4.526238	3.84
S12	239.5132	187.9587	123.7377	20.86
S13	12.85072	23.27216	4.358571	3.57
S14	12.77303	22.85079	4.325905	3.59
S15	12.3302	20.84518	3.914381	3.31
S16	112.7807	60.56923	7.045286	6.49
S17	12.2194	19.92979	3.784381	3.23
S18	0.264853	3.870574	0.87619	0.75
S19	12.38415	21.48498	4.159571	3.42
S20	12.32889	20.65336	3.995905	3.26
Min	0.264853	3.870574	0.87619	0.75
Max	1692.808	1308.148	123.7377	24.23
Average	365.5696	211.5803	22.24225	10.60591

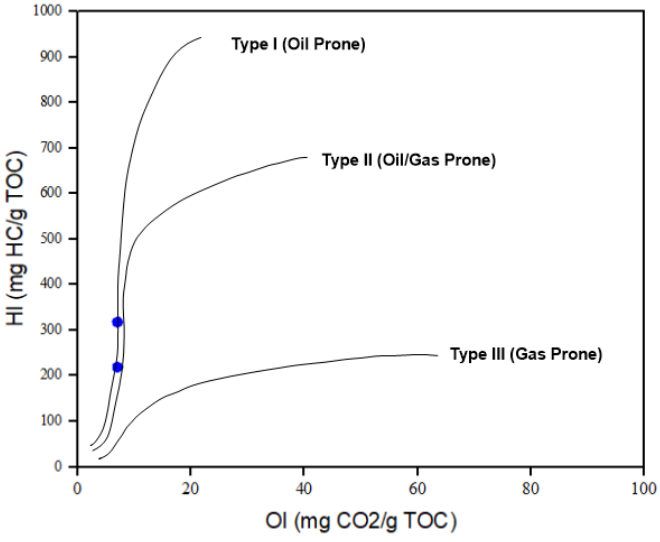

Figure 10. Plot of OI *vs* HI.

3.1.1. Exposed section in Akunza Mighili coal mine

The exposed section in the Akunza Mighili coal mine (N 8° 25' 40.3" E8° 34' 16.9") consists of shale interbedded with coal seams (Figure 4). The coal seams have a very dark appearance. In hand specimens, the coal samples vary in terms of their texture. However, the majority are very fine-grained. The samples are equally characterized by varying densities and moderate brittleness. In a few coal samples, especially those interbedded with very thin layers of sand and silt materials, quartz grains and clay minerals are very conspicuous. The shale appears greyish-yellow and fine-grained (Figure 4), with a well-developed thin plane, giving it adequate fissility and a smooth texture. Fossils were not observed in the shale. However, there are occasional infiltrations of plant roots.

3.1.2. Exposed section at Agyragu road

The section consists of a weathered shale exposed in a stream channel (N8° 27' 26.7", E8° 32' 32.6"). It exhibits a pale-greenish coloration with rusty red patches (Figure 5). The intensive weathering has obscured the shale's fissility resulting in friable and crumbly surfaces.

3.1.3. Mudstone

The mudstone occurs in the northeastern portion of the area. Despite its presence, the mudstone remains unmapped on the selected base map scale. It exhibits a very fine-grained to almost glassy texture with dark grey to black coloration. The surface conditions of the mudstone also showed that it has undergone significant weathering.

3.1.4. Ferruginous sandstone

Ferruginous sandstone covers a large area in the northern part of the study area. An exposure observed at latitudes 8° 28' 00"N to 8° 28' 50"N and longitudes 8° 32' 45"E to 8° 34' 15"E exhibits a reddish-brown coloration due to its high iron oxide content. It is medium-grained, dense, and durable, with well-sorted, sub-rounded quartz grains (Figure 6).

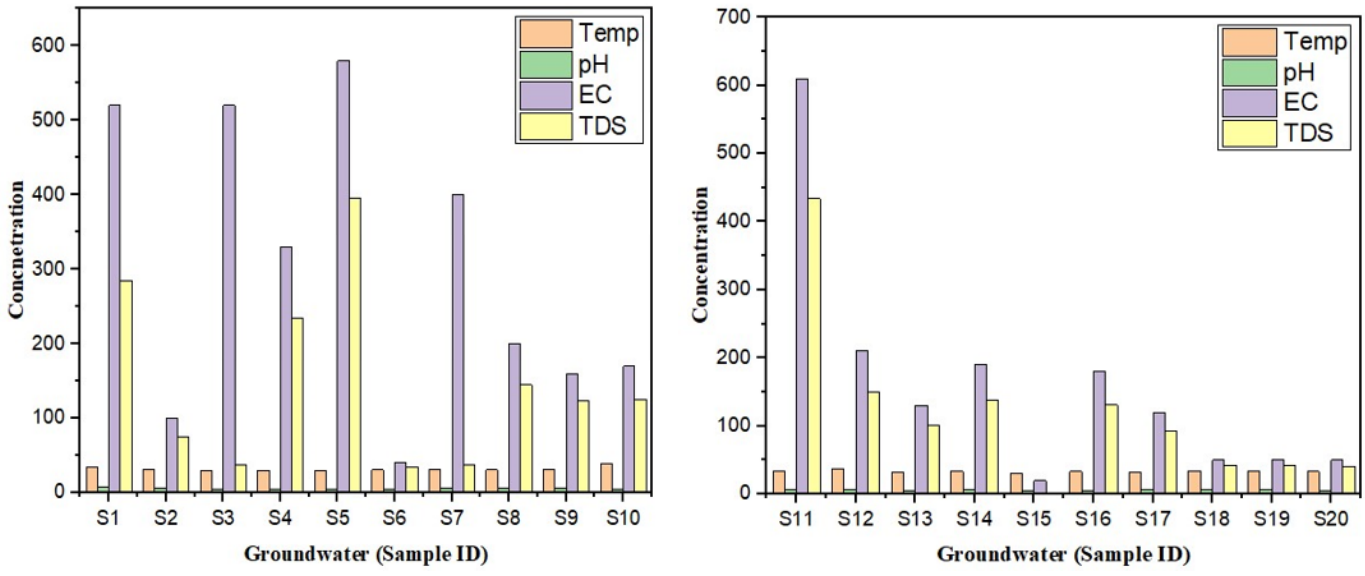

Figure 11. Concentration of the physical parameters.

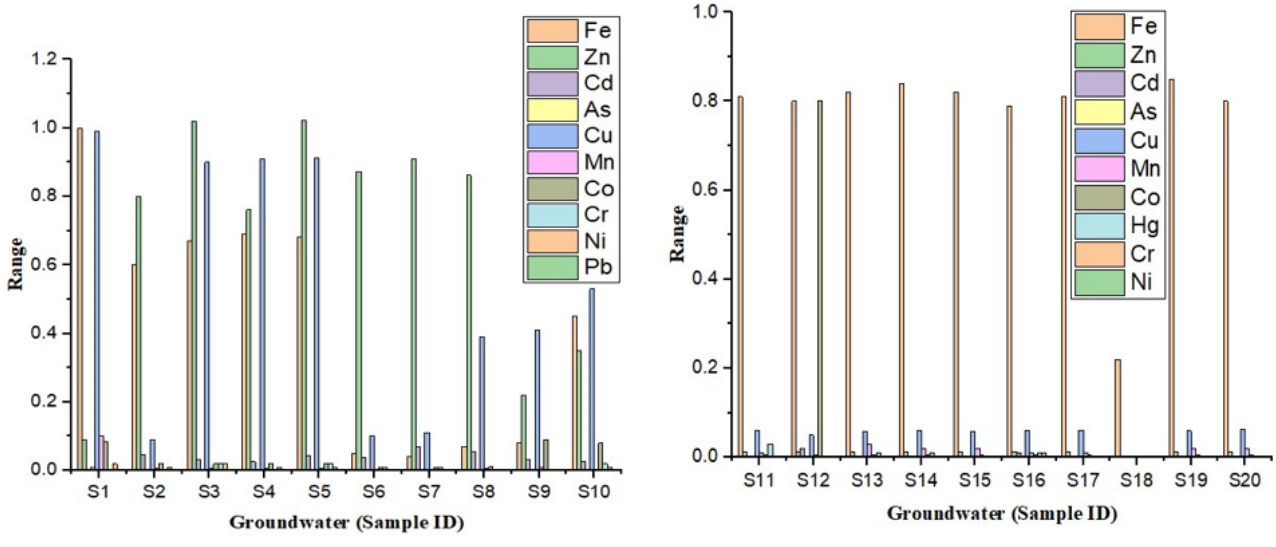

Figure 12. Concentration of the chemical parameters.

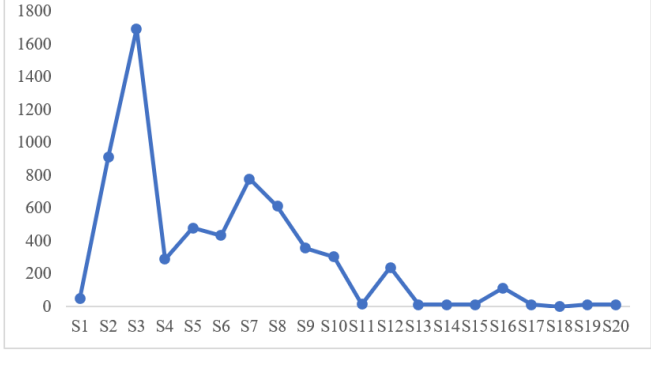

Figure 13. HPI values in groundwater samples of the area.

3.1.5. Ferruginous siltstone

The ferruginous siltstone also contains significant iron. In a few locations within the southeastern part of the area, it occurs as thin beds overlain by silt-sized materials (Figure 7A), while others mostly exhibit a reddish-brown coloration with a few yellowish-light patches. The ferruginous siltstone showed dominant quartz grains of varying silt sizes, cemented by iron oxide (Figure 7B).

3.2. WHOLE-ROCK GEOCHEMISTRY

The bulk chemical data for rocks in the area is presented in Table 1. The SiO_2 content ranges between 27.97 and 55.97 wt.% with an average of 42.70wt.%. Shale accounts for the highest SiO_2 content (55.97wt.%), followed by sandstone (49.45wt.%), mudstone (48.78wt.%), siltstone (31.78 wt.%), and coal (27.97wt.%). The average content of Fe_2O_3 in the sampled rocks is 27.06 wt.%, with the highest content occurring in the ferruginous sandstone,

ferruginous siltstone and mudstone with wt.% values of 52.33, 40.17 and 20.46 respectively. This result indicates a high iron content in the rocks, which translates to 52.33 wt.% Fe_2O_3 in oxide form, confirming their ferruginous nature. The Fe_2O_3 content in shale and coal is 13.15 wt.% and 9.19 wt.%, respectively. Al_2O_3 ranges between 8.06 and 21.76 wt.% with an average of 14.85 wt.%. The moderate amounts of Al_2O_3 coupled with the significant amounts of SiO_2 suggest the presence of aluminosilicate minerals in the sampled rocks. The K_2O concentration ranges between 0.02-2.94wt.% with an average of 1.46wt.%. MgO content is below detection in 83.3% of rock samples. However, coal shows 6 wt.%. The average concentration of P_2O_5 is 0.49 wt.% with values ranging between 0.15 and 0.83 wt.%. For CaO, the wt.% values vary from 0.08 to 8.26, averaging at 2.07 wt.%. MnO and TiO_2 range from 0.02-0.31 wt.% with an average of 0.176 wt.% and 0.39 to 4.1 wt.% with an average of 2.544 wt.%, respectively.

The X-Ray Fluorescence (XRF) results also showed a high SO3 content of 30.26 wt.% in the coal samples. SO3 content in the remaining rocks occurs in minor amounts ranging from 0.18 to 3.16 wt.% with an average of 6.92 wt.%. V_2O_3, Cr_2O_3, Ag_2O, BaO, CuO, Nb_2O_3, Ta_2O_5, SnO_2, ZrO_2, and ZnO showed average concentrations in trace amounts in all sampled rocks (Table 1).

The sandstone sample in the study area falls under the arkose field (Figure 8A), according to the sandstone classification diagram of Fe_2O3+MgO – Na_2O – K_2O by Blatt *et al.* [46]. Similarly, the log of (Fe_2O3/MgO) versus (SiO_2/Al_2O_3), based on Herron [47], indicated that mudstone and shale are plotted within the Fe-shale field, while sandstone is positioned within the Fe-sandstone field (Figure 8B), which aligns with the chemical composition of the rocks. The Blatt *et al.* [46] classification diagram considers only sandstones, while the Herron [47] classification considers sandstone and other clastic rocks.

3.3. MINERALOGY

The result of the rocks' bulk mineralogy is presented in Table 2. Graphite account for the dominant mineral in coal (40%). Graphite is a crystalline form of carbon; therefore, this indicates that the coal in the study area has high carbon content. The high percentage of carbon also suggests a high-ranked coal that has undergone prolonged period of organic matter maturation. Quartz accounts for 26% of the bulk mineralogy in the coal. It is considered a detrital impurity in coal, possibly derived from detrital inputs and primary mineralization processes. The high percentage of quartz aligns with the SiO_2 content in the coal as revealed by the XRF result (Table 1). The presence of epsomite (10.1%) indicates influences from secondary alteration of sulphide minerals, possibly due to water-rock interaction. Anhydrite constitutes 13.9% of the coal mineralogy. This contributed to the high SO_3 content in the coal as revealed by the XRF result (Table 1). Alunogen accounts for 9% of the bulk mineralogy, while epsomite occurs in minor amounts (0.8%) (Table 2).

Quartz is the dominant mineral in shale, accounting for 54% of bulk mineralogy (Table 2, Figure 7B). This indicates the shale is siliceous in nature, suggesting a significant detrital input, probably from sandstone. Orthoclase represents 27% while goethite and anatase constitute 13.5% and 5.9%, respectively. In mudstone, quartz accounts for 52% of the bulk minerals: anatase (6%), goethite (10%), orthoclase (22%) and anhydrite (9%) (Table 2).

The result of bulk rock mineralogy also revealed the dominance of goethite (iron oxide), moderate- significant percentage of quartz in the ferruginous sandstone and ferruginous siltstone samples in the study area. The goethite constitutes 58% in ferruginous sandstone, which conforms with the high iron content revealed in the XRF results (Table 1). The XRD result further indicates that the sandstone formed in a strong oxidizing condition, likely in an iron-rich fluvial or marine environment, and prolonged/extensive post-depositional chemical weathering. The significant content of quartz (27%) and a moderate amount of orthoclase (13.6%) contribute to the siliceous and feldspathic nature of the sandstone. Anatase occurs in minor amounts, constituting (1.6%). In the ferruginous siltstone, goethite accounts for the dominant mineral (53%). Quartz is significantly present (40%), with a minor amount of microcline (7.4%).

3.4. COAL PYROLYSIS

The coal pyrolysis was conducted on two representative coal samples to offer information about the coal's rank, thermal maturity, and hydrocarbon generation potential. The results of the coal pyrolysis, as presented in Table 3, indicate that the TOC values for coal samples from the area ranged from 64.97 wt.% to 70.31 wt., with a mean of 67.64 wt.%, while the free volatile hydrocarbon (*S1*), expressed in mg HC/g rock, ranged from 0.28 to 1.42, with a mean of 0.85. The *S2* (Pyrolysable hydrocarbon) ranged from 153.21 (mg HC/g rock) to 240.62 (mg HC/g rock) with an average of approximately 192.92 mg HC/g rock. The TOC values of coal in the area showed the coal samples are potential source rocks with excellent organic matter content when plotted against the *S2* in line with the [48, 49] classification (Figure 9). The TOC vs *S2* was further used to identify the quality and kerogen type in the coal samples [49–51]. The plot revealed that the coal samples fall within the Type II - Type II/III kerogen, which conforms with the oil-prone and mixed regions, respectively (Figure 11). Similarly, the relationship between the Oxygen Index (OI) and Hydrogen Index (HI), plotted on the modified Van Krevelen diagram [49, 52], also indicated that the coal samples are positioned within the Type II/Type III kerogen, which aligns with fairly poor gas-prone/good oil/gas-prone (Figure 10).

The thermal maturity of rocks was determined using the T_{max} (°C). The pyrolysis temperature depicts where the rate of hydrocarbon evolution reaches a maximum temperature (T_{max}) in a coal sample. In the research area, the T_{max} values range between 405°C for sample CS2 and 409°C for sample CS1. However, according to Espitalié *et al.* [48] and Anzaku *et al.* [51], the T_{max} of coal must be greater than 435°C before its maturation level can reach the oil generation threshold. This suggests the coal samples from the study area are immature for oil generation based on their T_{max} values.

3.5. PHYSICOCHEMICAL CHARACTERISTICS OF GROUNDWATER

The measured physical and chemical parameters of water samples are presented in Table 4. The World Health Organization [43] and the Standard Organization of Nigeria [53] water qual-

Table 6. Degree of contamination data of the groundwater

Sample ID	Zn	Cu	Hg	Cr	Fe	Co	Mn	Cd	Pb	As	Ni
S1	0.03	0.99	0.00	0.00	3.33	1.21	0.50	1.00	0.10	1.00	0.29
S2	0.27	0.09	0.00	0.00	2.00	0.30	0.03	15.33	0.00	0.00	0.14
S3	0.34	0.90	0.00	0.40	2.23	0.29	0.03	10.33	0.00	0.00	0.29
S4	0.25	0.91	0.00	0.00	2.30	0.30	0.03	8.67	0.00	0.00	0.14
S5	0.34	0.91	0.00	0.40	2.27	0.29	0.03	14.33	0.00	0.00	0.14
S6	0.29	0.10	0.00	0.20	0.17	0.14	0.00	13.00	0.00	0.00	0.00
S7	0.30	0.11	0.00	0.20	0.13	0.14	0.00	23.33	0.00	0.00	0.00
S8	0.29	0.39	0.00	0.00	0.23	0.16	0.04	18.33	0.00	0.00	0.00
S9	0.07	0.41	0.00	0.00	0.27	1.29	0.04	10.67	0.00	0.00	0.00
S10	0.12	0.53	0.00	0.40	1.50	1.14	0.02	9.00	0.10	0.00	0.14
S11	0.00	0.06	0.00	0.60	2.70	0.07	0.05	0.33	0.00	0.00	0.01
S12	0.00	0.05	0.00	0.00	2.67	11.43	0.03	6.67	0.00	0.00	0.01
S13	0.00	0.06	0.00	0.20	2.73	0.07	0.15	0.33	0.00	0.00	0.01
S14	0.00	0.06	0.00	0.20	2.80	0.07	0.10	0.33	0.00	0.00	0.01
S15	0.00	0.06	0.00	0.00	2.73	0.06	0.10	0.33	0.00	0.00	0.01
S16	0.00	0.06	0.00	0.20	2.63	0.06	0.05	3.33	0.00	0.00	0.14
S17	0.00	0.06	0.00	0.00	2.70	0.06	0.05	0.33	0.00	0.00	0.01
S18	0.00	0.00	0.00	0.00	0.73	0.01	0.00	0.00	0.00	0.00	0.00
S19	0.00	0.06	0.00	0.00	2.83	0.07	0.10	0.33	0.00	0.00	0.01
S20	0.00	0.06	0.00	0.00	2.67	0.07	0.10	0.33	0.00	0.00	0.01
Min.	0.00	0.00	0.00	0.00	0.13	0.01	0.00	0.00	0.00	0.00	0.00
Max.	0.34	0.99	0.00	0.60	3.33	11.43	0.50	23.33	0.10	1.00	0.29
Average	0.12	0.29	0.00	0.14	1.98	0.86	0.07	6.82	0.01	0.05	0.07

ity standards were compared with the measured parameters for relative assessment.

3.5.1. Physical parameters

The measured temperature (T) of groundwater varies between 29.9-38.0°C. The pH of the groundwater ranged from 4.5 to 8.6, indicating slightly acidic to alkaline conditions, with an average value of 5.9. The average concentration of the EC in the groundwater of the study area is 0.232.9mS/cm, with range values between 0.02-0.61mS/cm. All groundwater samples exhibited low to moderate concentrations of electrical conductivity, except for sample 11, which displayed a relatively higher concentration of 0.61 mS/cm, suggesting the influence of local anthropogenic factors [54]. The Total Dissolved Solid (TDS) values range from 0.22-434 mg/L with an average of 133.42mg/L. Following Todd's [55] TDS concentration-based water quality classification, the groundwater in the study area is classified as fresh, with TDS values < 1000 mg/L. Generally, the measured physical parameters (T, pH, EC, and TDS) showed concentration levels that were lower than the WHO [43] and SON [53] recommended standards. Figures 12A and B show the concentration of the physical parameters measured in the study area.

3.5.2. Chemical parameters

The chemical data of groundwater in the area (Table 4) revealed the mean concentration of trace elements in the order of Fe > Zn > Cu > Co > Cd > Mn > Cr > Ni > Pb > Hg. Fe ranges from 0.04 to 1 mg/L, with 75% of groundwater samples showing high concentrations greater than the recommended limits (0.3 mg/L) by WHO [43] and SON [53], respectively. This high iron content in the groundwater is attributed to the chemical and mineralogical composition of underlying rocks, which are excessively rich in iron oxides (Tables 1 and 2). As a result of water-rock interaction, the groundwater becomes highly enriched with iron from the dissolution of these iron oxides [36].

The groundwater in the area generally showed low enrichment of zinc, with values ranging from below the detection level to 1.02 mg/L, with an average of 0.37 mg/L (Table 4). The presence of zinc in groundwater is naturally associated with the dissolution of sulphide ores, such as sphalerite (ZnS), silicate minerals, and carbonate rocks [56]. Slightly more than half of the groundwater showed elevated Cd concentration above the WHO [43] and SON [53] thresholds of 0.003mg/L. Leachate from phosphate fertilizer, cadmium-coated materials, and cadmium-based batteries serves as a significant source of cadmium in groundwa-

ter [57, 58]. Farming activities are one of the major land use practices in the area, which may have contributed significantly to the high concentration of Cd in the groundwater. This is in addition to possible sources from the Akunza Mighili coal mine. The concentration of As were below the detection limit in 95% of groundwater samples. Cu concentrations were below the limits of 2mg/L and 1mg/L recommended by WHO [43] and SON [53], respectively. The values range from 0.05 mg/L to 0.99 mg/L with an average of approximately 0.31mg/L. Mn has an average concentration of mg/L and a maximum value of mg/L, while Co ranges from 0.001mg/L to 0.8 mg/L with an average of 0.06 mg/L.

The concentration of Hg is below the detection limit in all samples. For hexavalent Cr $^{(IV)}$, half of the groundwater showed concentrations below the detection limit, while the remaining 50% of the groundwater showed concentrations above the recommended limits of 0.006mg/L and 0.001mg/L prescribed by WHO [43] and SON [53], respectively. Cr is naturally associated with iron-bearing minerals such as hematite (Fe_2O_3) and goethite (FeOOH), chromite ($FeCr_2O_4$) clay minerals and organic matter [59]. However, under prevailing oxidizing conditions, the $Cr^{(III)}$ is converted to a more toxic and mobile $Cr^{(IV)}$, which easily dissolves in groundwater [60]. Coal combustion, in addition to other sources from industries and phosphate-bearing fertilizers, is a notable anthropogenic source of Cr in groundwater [61]. The concentrations of Ni and Pb in all samples are within the recommended limits of 0.07 mg/L for Ni and 0.02 mg/L for Pb, as specified by WHO [43] and SON [53], respectively.

3.6. ENVIRONMENTAL IMPACTS OF COAL EXPLOITATION AND HEALTH RISKS

The Akunza Mighili coal mine occurs within the Agwu shale (Figure 4A). The mineral composition of shale and coal samples in the research area (Table 1) indicates a significant content of silicate minerals, graphite (carbon), iron oxide, and sulphate-bearing minerals. These minerals are significant sources of trace heavy metals in the environment. Additionally, coal exploitation contributes to air quality issues and the degradation of natural resources [9, 36].

3.6.1. Assessment of heavy metal pollution in groundwater

Heavy Metal Pollution Index (HPI)

The heavy Metal Pollution Index (HPI) is a suitable technique used to evaluate the collective impact of heavy metals on the groundwater [62, 63]. The calculated HPI values of groundwater in the area range from 0.26 to 1692.81, with an average of 365.57 (Table 5). These values indicate that 45% of groundwater demonstrates low pollution with heavy metals (HPI<50), while 55% shows considerably high heavy metal pollution (HPI>100). The data suggests high health risks in the groundwater, so it should not be considered for drinking purposes. Similar investigations conducted by [37, 64] have shown high levels of heavy metals in water sources within the coal mine. Figure 14 shows the variation in the HPI values of groundwater samples from the area.

Modified Heavy Metal Pollution Index (MHPI)

The MHPI allows more accurate evaluation of heavy metal pollution in groundwater [35–38]. The MHPI values of groundwater in the research range from 3.87–1308.15, with a mean value of 211.58 (Table 5). Based on the MHPI results, excellent water quality for ingestion was recorded in 40% of the groundwater (MHPI<50), while 10% of the groundwater falls within the satisfactory water quality class (mHPI 50-100). Similarly, poor (MHPI 100-200) and destitute (MHPI 200-300) water quality was recorded in 25% and 15% of the groundwater, respectively, while 10% falls into the unsuitable water category (MHPI>300). These results are consistent with the HPI findings reported previously from the Heavy Metal Pollution Index (HPI). The groundwater samples that demonstrated poor water quality were mostly collected from the coal mine proximal areas. However, a few samples collected from areas away from the coal mine also demonstrated significant poor quality, which may be due to localized anthropogenic factors and likely agricultural practices at the appraised sites [65, 66].

Degree of Contamination (DC)

The DC values (Table 6) indicate that Ni, Zn, Cu, Cr, Mn, Pb, and As showed low contamination levels in the groundwater, with the following sequence in order of increasing average abundance: Cu>Cr>Zn>Ni=Mn,>As>pb. Fe varies from 0.13-3.33 with an average of 1.98. These value ranges give rise to low, medium, and high heavy metal pollution in 25%, 70%, and 5% of the samples, respectively. Long-term exposure to excessive Fe in groundwater can lead to cancer and liver problems [67]. High pollution level was recorded in 5% of the groundwater with respect to Co (DC>3). Excessive exposure to cobalt through ingestion, dermal contact, and inhalation is associated with skin irritation and chronic respiratory diseases as well as gastrointestinal discomforts [68–71]. The average DC of Cd is 6.82, with values varying from 0.00-0.23.3. Slightly more than 50% of the groundwater samples showed high pollution levels. Exposure to Cd in drinking water is linked to chronic kidney disease [72].

The cumulative DC values (Table 5) of all heavy metals assessed demonstrated a significant high heavy metal pollution (DC>3) in 95% of the groundwater of the research area, with values varying from 0.75-24.24. This indicates a significant degree of heavy metal pollution in the area and potential health risks. This finding also conforms to recent research, which reported both carcinogenic and non-carcinogenic health risks in children and adults in the area [36].

Heavy Metal Evaluation Index (HEI)

The computed HEI values vary from 0.88-123.7, with an average of 22.24. According to the HEI result interpretation, 45% of the groundwater showed low heavy metal pollution, suggesting that it is potable for drinking. Medium heavy metal pollution was recorded in 20% of groundwater, and 35% of the groundwater showed high pollution of the analyzed heavy metals.

3.6.2. Coal combustion and greenhouse gas emission

Air pollution

Coal exploitation, beneficiation, and combustion facilitate the release of various air pollutants, such as particulate matter (PM),

volatile elements, and toxic trace metals, which pose serious health concerns [5, 11]. The bulk rock mineralogy of the coal sample (Table 2) revealed a significant carbon content (40%), which serves as a major source of energy [3]. Members of the Akunza Mighili community use these coal samples for various domestic purposes, including coal combustion for space heating. During coal combustion, various gases such as carbon dioxide (CO_2), carbon monoxide (CO), sulphur dioxide (SO_2), sulphur trioxide (SO_3), nitrogen dioxide (NO_2), and nitric oxide (NO) are being released into the atmosphere in the form of flue gas, smoke, and fine ash [73–75]. The emission of these gases has been attributed to health issues such as respiratory, cardiovascular, blood, and brain diseases [74, 76]. CO_2 and CO are both greenhouse gases (GHGs) that significantly contribute to climate change [77]. Additionally, partial combustion of coal potentially generates particulate matter (PM), volatile organic compounds (VOCs), and polycyclic aromatic hydrocarbons (PAHs) [78–80]. These atmospheric pollutants are well-known carcinogens [11, 74].

Emission of sulphur dioxide (SO_2) and acid rain formation

Sulfur in coal often occur as pyritic sulfur (sulfide), elemental sulfur, organic sulfur and sulfates [81–83]. The presence of sulfate bearing minerals (anhydrite and alunogen) have been reported in the Akunza Mighili coal (Table 2). In any case, when coal is combusted, the available sulfur is oxidized to produce SOx, primarily sulfur dioxide (SO_2). The sulfur dioxide (SO_2) produced can react with water vapor when released into the atmosphere to form sulfuric acid which consequently leads to acid rain [84]. Acid rain renders a wide range of environmental effects such disruption of aquatic ecosystem, and corrosion of buildings [84, 85]. Various toxic and non-toxic heavy metals such as Hg, Cd, Pb, Zn, Mn, Al, Fe can be mobilized in the soil during the acid rain which may further contaminates soil, agricultural products and water bodies [86, 87]. Consumption of polluted crops results in gradual accumulation of these heavy metals in body leading serious kidney diseases [74].

Silica dust

Table 2 revealed a high quartz content in coal (25%) and host shale (54%). During the coal exploitation processes, fine quartz particles are produced in the form of dust, which poses serious occupational and community health risks [12]. Continuous and prolonged inhalations of these fine quartz particles may result in chronic silicosis, a severe lung disease characterized by fibrosis and respiratory failure [88]. However, acute silicosis can develop as a result of short-time, intense exposure to quartz particles, which frequently results in death [6]. Exposure to silica is also attributed to lung cancer and Chronic Obstructive Pulmonary Disease (COPD) [88, 89].

Coal dust

Coal dust is composed of fine particles of carbon, silica, and other mineral components released during the exploitation, handling, and combustion of coal [12, 90]. Coal dust is a widely known pollutant that causes serious occupational hazards in coal mining and other related industries [12, 91]. Inhalation of coal dust leads to its gradual accumulation in the lungs, which consequently results in severe respiratory diseases [92]. Long-term exposures have been linked to several lung disorders, such as chronic bronchitis and the most common pneumoconiosis, typically known as 'black lung disease' or Coal Workers' Pneumoconiosis (CWP) [12, 75, 93].

The carbon content in coal is a major factor that determines the severity of pneumoconiosis [6]. Thus, coal samples with a high carbon content pose higher pneumoconiosis risks. From the result of XRD analysis (Table 2), it is clear that the Akunza Mighili coal is composed of high carbon content (40%). Consequently, the mine workers and community members, especially those living close to the mine, are vulnerable to pneumoconiosis in the short term. The quartz content in the coal and shale can also influence pneumoconiosis [12].

Acid Mine Drainage (AMD)

Acid Mine Drainage (AMD), associated with coal mining processes and tailings, is another environmental pollutant that contaminates soil and water bodies [4, 94]. The formation of acid mine drainage occurs when sulphide minerals in coal, primarily pyrite (Fe_2S), are exposed to water and oxygen, which leads to the production of sulphuric acid and the subsequent release of heavy metals in dissolved form [95]. The surface mining method used at the Akunza Mighili coal mine provides favorable conditions for the formation of acid mine drainage due to the presence of high atmospheric oxygen (O_2) and hydrogen (H^+). The presence of secondary sulphate minerals such as epsomite ($MgSO_4.7H_2O$), anhydrite ($CaSO_4$), and alunogen ($Al_2(SO_4)_3.16H_2O$) in the Akunza Mighili coal (Table 2) suggests a secondary consequence of pyrite oxidation and a direct indication of ongoing sulphide oxidation and acid mine processes [96].

Deforestation

Surface mining, particularly the opencast method, has negative impacts on natural topography, vegetation, and soil [97], as it requires clearing vegetation and removing topsoil. These activities consequently result in habitat loss, biodiversity, and soil degradation [98]. The removal of trees and vegetation makes soil susceptible to erosion and reduces agricultural productivity. It is also associated with reduced carbon storage sinks [99], leading to higher concentrations of carbon dioxide in the atmosphere [100]. Figure 8A and B show a wide area of land degraded by mining activities in Akunza Mighili.

4. CONCLUSION

The environmental and health impacts of coal mining activities in the Akunza Mighili coal mine have been investigated. Shale, coal seams, ferruginous sandstone, ferruginous siltstone, and minor occurrences of mudstone primarily underlie the research area. The bulk mineralogical and geochemical analysis of coal samples indicated that graphite is the dominant mineral, while major oxide compositions are in the order of SO_3>SiO_2>Al_2O_3>Fe_2O_3>CaO>Ta_2O_5, respectively. Based on the T_{max} results, coal samples from the study area are immature for oil generation. The measured physical parameters (T, pH, EC, and TDS) in groundwater samples have lower concentrations than WHO's [43] and SON's [53] recommended standards.

The HPI result reveals that heavy metals pollute slightly more than half of the groundwater, potentially posing health hazards. Similarly, the MHPI result showed that 40% of the groundwater mainly collected from areas close to the coal mine exhibits poor water quality due to heavy metal pollution. Residents of the Akunza Mighili community and coal mine workers are vulnerable to respiratory diseases, including chronic silicosis and pneumoconiosis.

DATA AVAILABILITY

No additional data was used beyond those presented in the submitted manuscript.

References

[1] A. Alhasan, I. Ozturk, M. F. Al-Zyoud & F. V. Bekun, "Coal consumption–environmental sustainability nexus in developed and developing major coal-consuming economies", Heliyon **10** (2024) e25619. https://doi.org/10.1016/j.heliyon.2024.e25619.

[2] M. Song, J. Chen, Y. Feng, S. Xu, S. Zhao & Q. Xing, "Global emissions from coal consumption", in China's coal consumption, emissions, and energy security, Resources, Climate and Sustainable Development Series, Springer, Singapore, 2025, pp. 131. https://doi.org/10.1007/978-981-99-3407-9_8.

[3] L. Li, Y. Lei & D. Pan, "Economic and environmental evaluation of coal production in China and policy implications", Nat. Hazards **77** (2015) 1125. https://doi.org/10.1007/s11069-015-1644-9.

[4] S. Goswami, "Impact of coal mining on environment", European Researcher **92** (2015) 185. https://doi.org/10.13187/er.2015.92.185.

[5] P. Gopinathan, T. Subramani, S. Barbosa & D. Yuvaraj, "Environmental impact and health risk assessment due to coal mining and utilization", Environmental Geochemistry and Health (2023). https://doi.org/10.1007/s10653-023-01744-z.

[6] S. I. Chibuisi, "Environmental and health implications of coal mining at Maiganga, Gombe State, Nigeria", Journal of Environmental Pollution and Human Health **5** (2017) 1. https://doi.org/10.12691/jephh-5-1-2.

[7] I. L. Oltean, T. Goldan & C. M. Nistor, "Prevention and monitoring environmental impact of open pit coal mining activities", Research Journal of Agricultural Science **50** (2018) 259. https://rjas.ro/wp-content/uploads/2018/07/38.pdf.

[8] M. Davies, "Assessment of the impact of mining activities on land use and land cover changes in Gatumba area, Rwanda", International Journal of Innovative Science and Research Technology **8** (2023) 723. https://ijisrt.com/assessment-of-the-impact-of-mining-activities-on-land-use-and-land-cover-changes.

[9] S. Goswami, "Environmental impact assessment of coal mining: Indian scenario", European Researcher **83** (2014) 1651. https://doi.org/10.13187/er.2014.83.1651.

[10] R. O. Mkpuma, O. C. Okeke & E. M. Abraham, "Environmental problems of surface and underground mining: a review", International Journal of Engineering Science **4** (2015) 12. https://www.theijes.com/papers/vol4-issue12/Version-1/C0412012020.pdf.

[11] R. B. Finkelman, "Potential health impacts of burning coal beds and waste banks", International Journal of Coal Geology **59** (2004) 19. https://doi.org/10.1016/j.coal.2003.11.002.

[12] C. Kamanzi, M. Becker, M. Jacobs, P. Konečný, P. von Holdt & J. Broadhurst, "The impact of coal mine dust characteristics on pathways to respiratory harm: investigating the pneumoconiotic potency of coals", Environmental Geochemistry and Health (2023). https://doi.org/10.1007/s10653-023-01583-y.

[13] D. Jin & Z. Bian, "Quantifying the emissions impact of coal mining activities on the environment and human health", Journal of Coal Science and Engineering **19** (2013) 421. https://doi.org/10.1007/s12404-013-0405-2.

[14] M. Bortolotti, L. Lutterotti & G. Pepponi, "Combining XRD and XRF analysis in one Rietveld-like fitting", Powder Diffr. **32** (2017) S225. https://doi.org/10.1017/S0885715617000276.

[15] T. Radu & D. Diamond, "Comparison of soil pollution concentrations determined using AAS and portable XRF techniques", Journal of Hazardous Materials **171** (2009) 1168. https://doi.org/10.1016/j.jhazmat.2009.06.062.

[16] V. Singh & H. M. Agrawal, "Qualitative soil mineral analysis by EDXRF, XRD and AAS probes", Radiation Physics and Chemistry **81** (2012) 1796. https://doi.org/10.1016/j.radphyschem.2012.07.002.

[17] A. M. Abdelgawad, K. Watanabe, S. Takeuchi & T. Mizuno, "The origin of fluoride-rich groundwater in Mizunami area, Japan—mineralogy and geochemistry implications", Engineering Geology **108** (2009) 76. https://doi.org/10.1016/j.enggeo.2009.06.016.

[18] D. P. Singh & N. Sharma, "Heavy metal pollutants in water and their detection techniques", International Journal of Chemical Studies **9** (2021) 669. https://www.chemijournal.com/archives/2021/vol9issue1/PartK/9-1-144-921.pdf.

[19] S. Cornaby *et al.*, "An XRD/XRF instrument for the microanalysis of rocks and minerals", Measurement Science and Technology **12** (2001) 676. https://doi.org/10.1088/0957-0233/12/6/304.

[20] B. N. Hupp & J. J. Donovan, "Quantitative mineralogy for facies definition in the Marcellus Shale (Appalachian Basin, USA) using XRD–XRF integration", Sedimentary Geology **371** (2018) 16. https://doi.org/10.1016/j.sedgeo.2018.04.007.

[21] O. B. Kaba, F. Souissi, D. Keita, L. O. Filippov, M. S. M. Conté & N. Kanari, "Mineral weathering and metal leaching under meteoric conditions in F-(Ba–Pb–Zn) mining waste of Hammam Zriba (NE Tunisia)", Materials **16** (2023) 7443. https://doi.org/10.3390/ma16237443.

[22] A. Kamata & M. Katoh, "Arsenic release from marine sedimentary rock after excavation from urbanized coastal areas: oxidation of framboidal pyrite and subsequent natural suppression of arsenic release", Sci. Total Environ. **670** (2019) 752. https://doi.org/10.1016/j.scitotenv.2019.03.217.

[23] D. A. Purwaningsih, I. W. Redana, K. D. Harmayani & N. N. Pujianiki, "Evaluation of the potential for acid mine drainage formation from pit lake walls and its interaction with the aquifer system", J. Penelit. Pendidik. IPA **11** (2025) 839. https://doi.org/10.29303/jppipa.v11i5.11057.

[24] E. Marguí, I. Queralt & E. de Almeida, "X-ray fluorescence spectrometry for environmental analysis: basic principles, instrumentation, applications and recent trends", Chemosphere **303** (2022) 135006. https://doi.org/10.1016/j.chemosphere.2022.135006.

[25] Y. A. Uvarova, J. S. Cleverley, A. Baensch & M. Verrall, "Coupled XRF and XRD analyses for rapid and low-cost characterization of geological materials in the mineral exploration and mining industry", EXPLORE Newsl. Assoc. Appl. Geochem. **162** (2014) 1. https://www.appliedgeochemists.org/images/stories/explore/EXPLORE_162.pdf.

[26] L. Findoráková, O. Šestinová, J. Hančul'ák, E. Fedorová & A. Zorkovská, "Assessment of sediment heavy metals pollution using screening methods (XRF, TGA/MS, XRPD and earthworms bioassay)", IOP Conf. Ser. Earth Environ. Sci. **44** (2016) 052024. https://doi.org/10.1088/1755-1315/44/5/052024.

[27] A. Haghighizadeh *et al.*, "Comprehensive analysis of heavy metal soil contamination in mining environments: impacts, monitoring techniques, and remediation strategies", Arab. J. Chem. **17** (2024) 105777. https://doi.org/10.1016/j.arabjc.2024.105777.

[28] V. S. Kanwar, A. Sharma, A. L. Srivastav & L. Rani, "Phytoremediation of toxic metals present in soil and water environment: a critical review", Environ. Sci. Pollut. Res. **27** (2020) 44835. https://doi.org/10.1007/s11356-020-10713-3.

[29] N. L. Binbol, "A climate of Nasarawa State: report of geographical perspective on Nasarawa State", Department of Geography, Nasarawa State University, Keffi, Nigeria, 2006.

[30] S. C. Mohammed & M. Ali, "Hydrogeochemistry of the Middle Benue Trough, Nigeria", J. Water Resour. Ocean Sci. **7** (2019) 70.

[31] C. S. Nwajide, "Sedimentation and paleogeography of the Central Benue Trough, Nigeria", in The Benue trough: structure and evolution, C. Ofoegbu (Ed.), Vieweg, Braunschweig, Germany, 1990, pp. 19.

[32] M. E. Offodile & R. A. Rayment, "Stratigraphy of the Keana–Awe area of the Middle Benue region of Nigeria", Bull. Geol. Inst. Univ. Uppsala NS **7** (1977) 37.

[33] N. Obaje, Geology and mineral resources of Nigeria, Springer, Berlin, Germany, 2009. https://doi.org/10.1007/978-3-540-92685-6.

[34] N. D. Umar, O. Igwe & I. G. Idris, "Evaluation and characterization of groundwater of the Maastrichtian Lafia formation, Central Benue Trough, Nigeria", J. Earth Syst. Sci. **128** (2019) 168. https://doi.org/10.1007/s12040-019-1199-1.

[35] S. E. Obrike, A. I. Saleh, S. Iyakwari, K. G. Anudu & A. I. Magaji, "Hydrogeochemical evaluation, quality, and health risk assessment of groundwater in crystalline basement aquifer in Keffi, Nigeria", Int. J. Energy Water Resour., 2023.

[36] S. Aliyu, "Hydrogeochemical processes and health risk assessment of groundwater within Federal University of Lafia and environs", M.Sc Thesis, Nasarawa State University, Keffi, Nigeria, 2024.

[37] O. R. Ekwule, G. D. Akpen & G. M. Ugbede, ''The effect of coal mining on the water quality of water sources in Nigeria'', Bartın Univ. Int. J. Nat. Appl. Sci. **2** (2019) 251.
[38] O. A. Opasola & E. Otto, ''Evaluation of heavy metal levels and contamination indices of groundwater sources in Kaduna South Local Government Area, Kaduna State, Northern Nigeria'', J Appl Sci Env. Manage **28** (2024) 1841.
[39] R. Appiah-Opong *et al.*, ''Heavy metals concentration and pollution index (HPI) in drinking water along the southwest coast of Ghana'', Appl. Water Sci. **11** (2021) 57. https://doi.org/10.1007/s13201-021-01386-5.
[40] A. E. Edet & O. E. Offiong, ''Evaluation of water quality pollution indices for heavy metal contamination monitoring: a study case from Akpabuyo-Odukpani area, Lower Cross River Basin, Southeastern Nigeria'', GeoJournal **57** (2002) 295.
[41] S. Mishra, A. Jumar, S. Yada & M. K. Singhal, ''Assessment of heavy metal contamination in water of Kali river using principle component and cluster analysis, India'', J Sustain Water Resour Manag, 2017. https://doi.org/10.1007/s40899-017-0141-4.
[42] S. V. Mohan, P. Nithila & S. J. Reddy, ''Estimation of heavy metals in drinking water and development of heavy metal pollution index'', J Env. Sci Health **2** (1996) 283.
[43] WHO, Guidelines for Drinking Water Quality: Fourth Edition Incorporating the First Addendum, Geneva, Switzerland, 2017.
[44] J. C. Egbueri, C. K. Ezugwu, P. D. Ameh & C. O. Unigwe, ''Appraising drinking water quality in Ikem rural area (Nigeria) based on chemometrics and multiple indexical methods'', Env. Monit Assess **193** (2020) 1. https://doi.org/10.1007/s10661-020-08277-3.
[45] M. A. Akpanowo, N. Benson, G. B. Ekong, I. Umaru, S. Iyakwari & S. D. Yusuf, ''Effect of artisanal mining on water quality: an assessment of water sources in local communities in Anka, Northwest Nigeria'', ISABB J. Health Environ. Sci. **10** (2025) 13. https://doi.org/10.5897/ISAAB-JHE2023.0085.
[46] H. Blatt, G. Middleton & R. Murray, Origin of Sedimentary Rocks, Prince Hall, 1980.
[47] M. M. Herron, ''Geochemical classification of terrigenous sands and shales from core or log data'', J. Sediment. Petrol. **58** (1988) 820.
[48] J. Espitalié, G. Deroo & F. Marquis, ''Rock-Eval pyrolysis and its applications'', Rev. Institut Français Pet. **40** (1985) 563. https://doi.org/10.2516/ogst:1986003.
[49] M. R. Shalaby, M. I. Haji Irwan, L. N. Osli & M. Aminul Islam, ''Geochemical characteristics and depositional environments of the Narimba Formation source rock, Bass Basin, Australia'', J. Pet. Explor. Prod. Technol., 2020. https://doi.org/10.1007/s13202-020-00992-4.
[50] F. F. Langford & M. M. Blanc-Valleron, ''Interpreting Rock-Eval pyrolysis data using graphs of pyrolizable hydrocarbons vs. total organic carbon'', AAPG Bull **76** (1990) 799.
[51] I. Y. Anzaku, T. B. Gbatse & N. G. Obaje, ''Biomarker and bulk organic geochemical analysis of hydrocarbon generative potentials of the Ahoko Shales, Patti Formation, Bida Basin, Central Nigeria'', DJOSTER **4** (2015) 1.
[52] B. P. Tissot & D. H. Welte, Petroleum Formation and Occurrence: A New Approach to Oil and Gas Exploration, Springer-Verlag, Berlin, 1978.
[53] SON, Nigerian Standard for Drinking Water Quality, Nigerian Industrial Standards, 2015.
[54] N. Subba Rao, Hydrogeology – Problems with Solutions, PHI Learning Private Limited, 2016.
[55] D. K. Todd, Groundwater Hydrology, Wiley, New York, 1980.
[56] B. J. Alloway, ''Sources of heavy metals and metalloids in soils'', in Heavy Metals in Soils, Dordrecht: Springer, 2013, pp. 11.
[57] K. Andreas, T. W. Richard & P. Thomas, ''Cadmium in soil and groundwater: a review'', Appl. Geochem. **108** (2019) 104388. https://doi.org/10.1016/j.apgeochem.2019.104388.
[58] C. Tokatli & F. Ustaoglu, ''Health risk assessment of toxicants in Meriç river delta wetland, Thrace region, Turkey'', Env. Earth Sci. **7** (2020) 1. https://doi.org/10.1007/s12665-020-09171-4.
[59] A. Kabata-Pendias & A. Mukherjee, Trace Elements from Soil to Human, Springer-Verlag, 2007.
[60] ATSDR, Toxicological Profile for Chromium, U.S Department of Health and Human Services, Public Health Service, 2012.
[61] P. Maria, Eleni Vasileiou & B. Georgios, ''Tracing the origin of chromium in groundwater: current and new perspectives'', Curr. Opin. Environ. Sci. Health **22** (2021) 100267. https://doi.org/10.1016/j.coesh.2021.100267.
[62] R. Ali, H. Hossein, H. Sara, J. Nima, F. M. Seyedah Belgheys & Samira Rezaei, ''Evaluation of groundwater quality and heavy metal pollution indices in Bazman Basin, Southeastern Iran'', Groundw. Sustain. Dev. **9** (2019) 100245. https://doi.org/10.1016/j.gsd.2019.100245.
[63] V. Sheykhi & F. Moore, ''Geochemical characterization of Kor River water quality, Fars Province, South Iran'', Water Qual. Expo Health **4** (2012) 25. https://doi.org/10.1007/s12403-012-0063.
[64] C. I. Umoru, A. S. Atodo, A. S. Usman, S. Abdulrahman & C. Bitrus, ''The impact of coal mining on water around Okobo and Odagbo area, Ankpa, North-Central Nigeria'', FUDMA J. Sci. **8** (2024) 550. https://doi.org/10.33003/fjs-2024-0806-3018.
[65] A. Rashid *et al.*, ''Heavy metal contamination in agricultural soil: environmental pollutants affecting crop health'', Agronomy **13** (2023) 1521. https://doi.org/10.3390/agronomy13061521.
[66] W. Xu, Y. Jin & G. Zeng, ''Introduction of heavy metals contamination in the water and soil: a review on source, toxicity and remediation methods'', Green Chem. Lett. Rev. **17** (2024) 2404235. https://doi.org/10.1080/17518253.2024.2404235.
[67] WHO, World Health Organization End of Year Report, Geneva, 2003.
[68] ATSDR, Toxicological Profile for Cobalt, U.S Department of Health and Human Services, Public Health Service, 2020.
[69] IARC, Cobalt in hard metals and cobalt sulfate, Gallium Arsenide, Indium Phospide and Vanadium Pentoxide, IARC Monograph on the Evaluation of Carcinogenic Risks to Humans, 2006.
[70] L. Leyssens, B. Vinck, C. Van Der Straeten, F. Wuyts & L. Maes, ''Cobalt toxicity in humans – a review of the potential sources and health effects'', Toxicology **387** (2017) 43. https://doi.org/10.1016/j.tox.2017.05.015.
[71] A. Linna, P. Oska, P. Palmroos, P. Roto, P. Laippala & J. Uitti, ''Respiratory health of cobalt production workers'', Am J Ind Med **44** (2003) 124. https://doi.org/10.1002/ajim.10258.
[72] ATSDR, Toxicological Profile for Cadmium, U.S Department of Health and Human Services, Public Health Service, 2012.
[73] J. Chen *et al.*, ''Coal utilization in China: environmental impacts and human health'', Environ. Geochem. Health **36** (2014) 35.
[74] E. M. Muhammad, ''Human health and environmental impacts of coal combustion and post-combustion wastes'', J. Sustain. Min. **17** (2018) 87. https://doi.org/10.1016/j.jsm.2017.12.007.
[75] S. Mukherjee, ''Concept of geomedicine and medicinal mineralogy'', in Applied Mineralogy: Applications in Industry and Environment, New Dehli: Capital Publishing Company, 2011, pp. 526.
[76] D. G. Badman & E. R. Jaffe MD, ''Blood and air pollution: state of knowledge and research needs'', Otolaryngol.-Head Neck Surg. **114** (1996) 205. https://doi.org/10.1016/S0194-5998(96)70166-3.
[77] IPCC, Climate Change 2021: The Physical Science Basis, Cambridge University Press, 2021.
[78] Y. Chen *et al.*, ''Spatiotemporal distribution, sources apportionment and ecological risks of PAHs: a study in the Wuhan section of the Yangtze River'', Environ. Geochem. Health, 2023. https://doi.org/10.1007/s10653-023-01500-3.
[79] N. Mahlangeni, T. Kapwata, T. Laban & C. Y. Wright, ''Health risks of exposure to air pollution in areas where coal-fire power plants are located: protocols for scoping review'', **19** (2024) 1. https://doi.org/10.1136/bmjopen-2024-084074.
[80] Y. Qian, K. Yuan, J. Wang, Z. Xu, H. Liang & C. Tie, ''Parent and alkylated polycyclic aromatic hydrocarbon emissions from coal seam fire at Wuda, Inner Mongolia, China: characteristics, spatial distribution, sources, and health risk assessment'', Environ. Geochem. Health, 2023. https://doi.org/10.1007/s10653-023-01476-0.
[81] C. Chen-Lin, ''Sulfur in coals: a review of geochemistry and origins'', Int. J. Coal Geol. **100** (2012) 1. https://doi.org/10.1016/j.coal.2012.05.009.
[82] B. Ryan & L. Angelo, ''A review of sulphur in coal: with specific reference to the Telkwa deposit, North-Western'', Br. Columbia Geol. Fieldwork, (1997) 1998.
[83] Y. Shen, Y. Hu, M. Wang, W. Bao, L. Chand & K. Xie, ''Speciation and thermal transformation of sulfur-coal and its utilization in coal-blending coking process: a review'', Chin. J. Chem. Eng., 2021. https://doi.org/10.1016/j.cjche.2021.04.007.
[84] G. Twagirayezu *et al.*, ''A critical review of acid rain: causes, effects, and mitigation measures'', Nov. Perspect. Geogr. Environ. Earth Sci. **6** (2024) 23. https://doi.org/10.9734/bpi/npgees/v6/5127A.
[85] P. Sedyaaw *et al.*, ''A review on acid rain, its causes, effects and management measures'', Int. J. Creat. Res. Thoughts **12** (2024) 959.
[86] M. Scheiber, M. Otto, P. S. Fedotov & R. Wennrich, ''Dynamic studies on the mobility of trace elements in soil and sediment samples influenced

by dumping of residues of the flood in the Mulde River region in 2002'', Chemosphere **61** (2005) 107. https://doi.org/10.1016/j.chemosphere.2005.02.096.

[87] T. Arao, S. Ishikawa, M. Murakami, K. Abe, Y. Maejima & T. Makino, ''Heavy metal contamination of agricultural soil and countermeasures in Japan'', Paddy Water Environ. **8** (2010) 247. https://doi.org/10.1007/s10333-010-0205-7.

[88] S. Sen, R. Mitra, S. Mukherjee, P. K. Das & S. Moittra, ''Silicosis in current scenario: a review of literature'', Curr. Respir. Med. Rev. **12** (2016) 56.

[89] E. Hnizdo & V. Vallyathan, ''Chronic obstructive pulmonary disease due to occupational exposure to silica dust: a review of epidemiological and pathological evidence'', Occup Env. Med **60** (2003) 237. https://doi.org/10.1136/oem.60.4.237.

[90] C. Zinman, G. A. Richards, J. Murray, J. I. Phillips, D. J. Rees & R. G. Thomas, ''Mica dust as a cause of severe pneumoconiosis'', Am. J. Ind. Med. **41** (2002) 139.

[91] DHHS, Coal Mine Dust Exposures and Associated Health Outcomes, Centers for Disease Control and Prevention National Institute for Occupational Safety and Health, 2011.

[92] R. Cohen, E. Petsonk, C. Rose, B. Young, M. Ragier & F. Green, ''Lung pathology in U.S. coal workers with rapidly progressive pneumoconiosis implicates silica and silicates'', American Journal of Respiratory and Critical Care Medicine **15** (2016) 673. https://stacks.cdc.gov/view/cdc/202233.

[93] E. Petsonk, C. Rose & R. Cohen, ''Coal mine dust lung disease. New lessons from old exposure'', Am J Respir Crit Care Med **1** (2013) 1178. https://doi.org/10.1164/rccm.201301-0042CI.

[94] C. J. B. Gomes, C. A. B. Mendes & J. F. C. L. Costa, ''The environmental impact of coal mining: a case study in Brazil's Sangao watershed'', Mine Water Environ. **30** (2011) 159.

[95] B. D. Johnson & B. K. Hallberge, ''Acid mine drainage remediation options: a review'', Sci. Total Environ. **338** (2005) 3. https://doi.org/10.1016/j.scitotenv.2004.09.002.

[96] J. M. Hammarstrom, R. R. Seal II, A. L. Meier & J. M. Kornfeld, ''Secondary sulfate minerals associated with acid drainage in the Eastern US: recycling of metals and acidity in surficial environments'', Chem. Geol. **215** (2005) 407. https://doi.org/10.1016/j.chemgeo.2004.06.053.

[97] J. Wang, L. Guo, Z. Bai, R. Yang & M. Zhang, ''Succession law of reclaimed soil and vegetation on opencast coal mine dump of Loess area'', Trans. Chin. Soc. Agric. Eng **29** (2013) 223.

[98] Z. Bian, H. Inyang, J. L. Daniels, F. Otto & S. Struthers, ''Environmental issues from coal mining and their solutions'', Min. Sci. Technol. China **20** (2010) 215. https://doi.org/10.1016/S1674-5264(09)60187.

[99] Y. Huang, F. Tian, Y. Wang, M. Wang & Z. Hu, ''Effect of coal mining on vegetation disturbance and associated carbon loss'', Env. Earth Sci **73** (2015) 2329. https://doi.org/10.1007/s12665-014-3584-z.

[100] A. Roy, ''Impact of coal mining on vegetation'', Int. J. Ecol. Environ. Sci. **4** (2022) 74.